HEFAT2014
10th International Conference on Heat Transfer, Fluid Mechanics and Thermodynamics
14 – 16 July 2014
Orlando, Florida

# NUMERICAL INVESTIGATION OF CONJUGATE FREE CONVECTION WITH SURFACE RADIATION FROM A LEFT VERTICAL WALL OF CLOSED/OPEN CAVITIES WITH UNIFORM VOLUMETRIC HEAT GENERATING SOURCE

Singh, S.N
Department of Mechanical Engineering
Indian School of Mines, Dhanbad
Jharkhand-826004
India
E-mail:snsingh631@yahoo.com

## ABSTRACT

The results of fundamental study of conjugate free convection and surface radiation from the left wall with uniform volumetric heat source in a two-dimensional open cavities with air as the intervening medium are reported. Modified Rayleigh numbers, $Ra^* = 5\times10^4 - 5\times10^6$, aspect ratios, A = 2 – 4, and Prandtl number, Pr = 0.71 have been considered in the present problem. The governing equations, written in terms of stream function –vorticity formulation, have been solved using a finite volume method. For surface radiation calculations, radiosity –irradiation formulation has been used, while the view factors required therein, are calculated using the Hottel's Crossed-string method. The effects of heat source, the material and surface properties of the left wall on both heat transfer and fluid flow have been studied. Based on a set of numerical data, a correlation has been developed for maximum non-dimensional left wall temperatures.

## INTRODUCTION

Pure free convection in open cavities has been extensively studied both numerically and experimentally by the earlier studies of Rodighiero and de Socio [1], Angirisa and Mahajan [2] and Abib and Jaluria [3]. In an open cavity there is a continuous intake of fresh air from the ambient and exhaust of heated air back to the ambient and hence stratification effects are reduced. On the contrary, a very strong stratification effects are observed in closed cavities as investigated by Kim and Viskanata [4], Ridouane and Hasnaoui [5] and many others. Singh[6] has investigated the interactions of pure natural convection in the closed cavities and presented many useful results. He has also developed empirical correlation in terms of convective Nusselt number which was not done by earlier studies by Ridouane and Hasnaoui [5].

In the recent past there has been a renewed interest in the present work because of its applications to cooling of electronic circuit boards, solar energy collection devices, air flow in rooms, double pane windows and so forth. Though very simple in design, this geometry presents interesting physics governing the flow and heat transfer from the walls that form the cavity. The radiative interaction among the walls of the cavity and its effect on natural convection heat transfer is of fundamental importance in the design of such systems. In natural convection systems, even moderate temperature differences give rise to significant radiation effects so that the radiative and convective contributions may become comparable and thus influence the total heat transfer rate. It is therefore unrealistic to ignore the interactions of surface radiation and natural convection in this geometry.

Conjugate natural convection and surface radiation in open cavities is of current interest as indicated by the recent study of G. Lauriat et al. [7]. In the first part of his study the conjugate problem of natural convection and wall conduction for various thermal resistances has been discussed while the effects of surface radiation are discussed in the second part of the paper. Earlier Lage et al.[8] numerically investigated the combined natural convection and surface radiation in a two-dimensional open top cavity with one side heated (left wall), one side (right wall) and bottom insulated. After that Balaji and Venkateshan [9], in the light of their study, pointed out that the numerical study by Lage et al.[8] did not properly model the flow and heat transfer interaction within the cavity. In addition, Balaji and Venkateshan [10, 11] highlighted the need for considering the multi-mode heat transfer interactions while modeling problems of these types. Dehghan and Behnia [12], Yu and Joshi [13], Gururaja Rao et al. [14], Ramesh et al. [15], Ramesh and Merzkirch [16] and Singh and Venkateshan [17, 18] analyzed the multi-mode heat transfer in partially open cavities.

Rao et al.[19] presented the effect of surface radiation on conjugate convection in closed and discretely heated rectangular cavity. Martysuushev and Sheremet[20] have recently investigated the conjugate natural convection combined with surface radiation in an air filled cavity with internal heat source.

While much progress has been accomplished in understanding the multi-mode heat transfer in open cavities, there are still some important areas requiring attention. However, to the best of my knowledge, the systematic studies in the area of the conjugate heat transfer and fluid flow in the present geometry has not been examined in detail. The present study has also given emphasis on the velocity boundary conditions used by investigations of Angirisa and Mahajan [2] and Abib and Jaluria [3] at the partial opening and concluded that those boundary conditions are not suitable in this work because of radiation heating of the side vent wall.

**NOMENCLATURE**

| | | |
|---|---|---|
| A | [-] | aspect ratio, H/d |
| $A_1$ | [-] | geometric ratio, d/t |
| d | [m] | pacing, m |
| $F_{ij}$ | [-] | view factor from $i^{th}$ to $j^{th}$ element |
| G' | [W/m$^2$] | dimensional radiosity, |
| G | [-] | elemental dimensionless irradiation, G'/$\sigma\ T_{ref}^4$ |
| H | [m] | height of the cavity |
| J' | [W/m$^2$] | dimensional radiosity |
| J | [-] | elemental dimensionless radiosity, J'/ $\sigma\ T_{ref}^4$ |
| k | [W / m-K] | thermal conductivity of the fluid |
| $k_s$ | [W / m-K] | thermal conductivity of the left wall |
| m | [-] | number of grid segments in Y-direction |
| n | [-] | number of grid segments in X-direction |
| $N_{rc}$, $N_{rf}$ | [-] | radiation conduction parameter or radiation flow parameter, $\frac{\sigma T_{ref}^4 d}{\Delta T_{ref} k}$ |
| Pr | [-] | Prandtl number, $\frac{\nu}{\alpha}$ |
| $q_v$ | [W/ m3] | uniform volumetric heat generation rate |
| Ra* | [-] | modified Rayleigh number, $\frac{g\beta\Delta T_{ref} H^3}{\nu^2} \times Pr$ |
| Ra | [-] | Rayleigh number, $\frac{g\beta\Delta T H^3}{\nu^2} \times Pr$ |
| t | [m] | thickness of the left wall |
| T | [K] | temperature of $i_{th}$ element, |
| $T_{ref}$ | [K] | reference temperature of the left wall of the cavity |
| u , v | [m/s] | dimensional vertical and horizontal velocity, |
| U, V | [-] | dimensioless vertical and horizontal velocities, $\frac{u d}{\alpha}$ and $\frac{v d}{\alpha}$ . |
| X,Y | [-] | dimensionless vertical and horizontal coordinates, x/d & y/d. |
| w | [m] | vent height |
| W | [-] | vent ratio, w/ H |

**Greek Letters**

| | | |
|---|---|---|
| $\alpha$ | [ m$^2$/s] | thermal diffusivity |
| $\beta$ | [1/K] | isobaric coefficient of volumetric expansion |
| $\varepsilon$ | [-] | emissivity of the walls |
| $\nu$ | [ m$^2$/s] | kinematic viscosity |
| $\gamma$ | [-] | thermal conductance parameter, $\frac{k\ d}{k_s\ t}$ |
| $\sigma$ | [ W/ m$^2$ K$^4$ ] | Stefan Boltzmann constant, $5.67 \times 10^{-8}$ |
| $\Delta T_{ref}$ | [K ] | modified reference temperature difference, |
| $\Theta$ | [-] | dimensionless temperature, ( T - $T_\infty$) / $\Delta T_{ref}$ |
| $\psi'$ | [ m$^2$/s ] | dimensional stream function, |
| $\Psi$ | [-] | dimensionless stream function, $\frac{\psi'}{\alpha}$ |
| $\omega'$ | [1/s] | dimensional vorticity |
| $\Omega$ | [-] | dimensionless vorticity, $\frac{\omega' d^2}{\nu}$ |

**MATHEMATICAL FORMULATION**

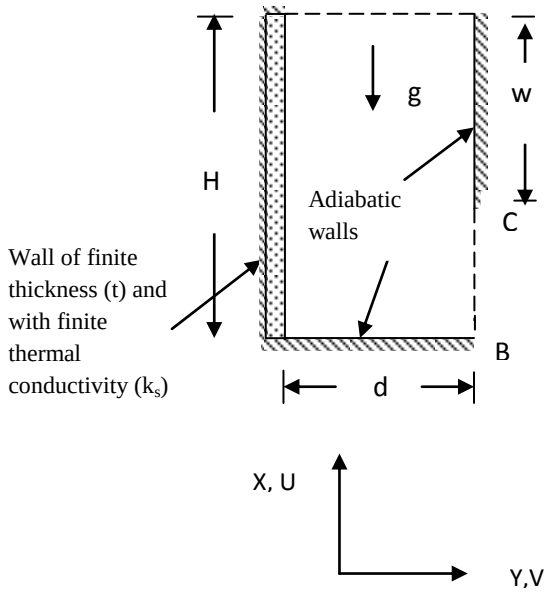


Fig. 1 Schematic geometry of the present problem

The conjugate free convection with surface radiation in a side vented open top cavity with having uniform heat generating left wall shown schematically in Fig.1, can be formulated as stream function and vorticity ($\omega - \psi$) form for a constant property fluid under the Boussinesq approximation, in non-dimensional form as

$$U\frac{\partial \omega}{\partial X} + V\frac{\partial \omega}{\partial Y} = Pr\left[\frac{\partial^2 \omega}{\partial X^2} + \frac{\partial^2 \omega}{\partial Y^2}\right] - Ra^*\frac{\partial \theta}{\partial Y} \quad (1)$$

$$\frac{\partial^2 \psi}{\partial X^2} + \frac{\partial^2 \psi}{\partial Y^2} = -\omega \times Pr \quad (2)$$

$$U\frac{\partial\theta}{\partial X}+V\frac{\partial\theta}{\partial Y}=\left[\frac{\partial^2\theta}{\partial X^2}+\frac{\partial^2\theta}{\partial Y^2}\right] \quad (3)$$

The enclosure method of analysis, with radiosity-irradiation formulation for the evaluation of the radiosities of all the wall elements, is used for surface radiation related calculations. The walls are assumed diffuse and gray. The general radiosity equation for the $i^{th}$ element of an enclosure may be written as

$$J_i = \varepsilon_i (T_i/T_{ref})^4 + (1-\varepsilon_i)\sum_{j=1}^{n} F_{ij} J_j \quad \text{for} [1 \le i \le n] \quad (4)$$

## BOUNDARY CONDITIONS

The boundary conditions are specified for stream function, vorticity and temperature on all the boundaries based on Singh and Venkateshan [17, 18] which are also given here except left wall temperature boundary condition which is given in Eq. (14).

Left vertical wall:

$$\psi=0,\ \omega=-\frac{1}{Pr}\frac{\partial^2\psi}{\partial Y^2} \quad (5)$$

Bottom wall:

$$\psi=0,\ \omega=-\frac{1}{Pr}\frac{\partial^2\psi}{\partial X^2},\ \frac{\partial\theta}{\partial X}=N_{rc}[J-G] \quad (6)$$

Side – vent wall:

$$\psi=C(\text{unknown}),\ \omega=-\frac{1}{Pr}\frac{\partial^2\psi}{\partial Y^2},\ \frac{\partial\theta}{\partial Y}=N_{rc}[J-G] \quad (7)$$

Along side opening, BC:

$$\frac{\partial U}{\partial X}=0,\ \frac{\partial V}{\partial Y}=0,\ \frac{\partial^2\psi}{\partial X\partial Y}=0\ (\text{Mixed velocity}),\ \omega=0,\theta=0 \quad (8)$$

Top- opening:

$$\frac{\partial\psi}{\partial X}=0,\ \frac{\partial\omega}{\partial X}=0,\ \theta=0 \text{ if } U<0,\ \frac{\partial\theta}{\partial X}=0 \text{ if } U>0 \quad (9)$$

The equation for temperature distribution along the left of the cavity wall is derived based on an energy balance of an enlarged wall element chosen from Fig. 1 as shown below.

$$Q_{cond,\,x} + q_v \Delta x\, t\times 1 = Q_{cond,\,(x+\Delta x)} + Q_{conv} + Q_{rad} \quad (10)$$

$$Q_{cond,\,x} + q_v \Delta x\, t\times 1 = \left[Q_{cond} + \frac{\partial Q_{cond,\,x}}{\partial x}\Delta x\right] + \left[-k\frac{\partial T}{\partial y}(\Delta x\times 1)\right] + \left[\frac{\varepsilon}{1-\varepsilon}\right](\sigma T^4 - J')(\Delta x\times 1) \quad (11)$$

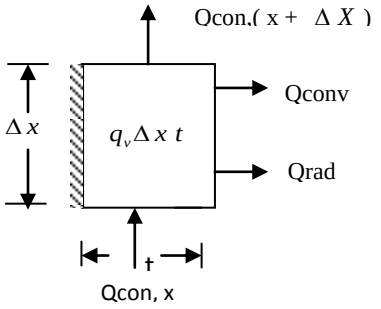


$$q_v\, t = \frac{\partial}{\partial x}\left(-k_s\frac{\partial T}{\partial x}(t\times 1)\right) - k\left(\frac{\partial T}{\partial y}\right)_{y=0} + \left[\frac{\varepsilon}{1-\varepsilon}\right](\sigma T^4 - J') \quad (12)$$

$$k_s\, t\left(\frac{\partial^2 T}{\partial x^2}\right) + k\left(\frac{\partial T}{\partial y}\right)_{y=0} + q_v\, t - \left[\frac{\varepsilon}{1-\varepsilon}\right](\sigma T^4 - J') = 0 \quad (13)$$

The above equation, after simplification and non-dimensionalization, results in the following equation for temperature distribution along the left wall :

$$\frac{\partial^2\theta}{\partial X^2} + \gamma\left(\frac{\partial\theta}{\partial Y}\right)_{Y=0} + \left(\frac{A_1}{A}\right) - \left(\frac{\varepsilon}{1-\varepsilon}\right)\gamma N_{rf}\left[\left(\frac{T}{T_{ref}}\right)^4 - J\right] = 0 \quad (14)$$

However, heat transfer in the conducting – heat generating left wall is treated as a convecting – radiating "fin" problem as given in equation (10). Equation (14) gets appropriately modified for the insulated bottom and top ends of the left wall.

## METHOD OF SOLUTION

The governing equations (1) - (3) are first transformed into finite difference equations using a finite volume based finite difference method of Gosman et al. [21]. The advection terms present in equations (1) and (3) are handled using a second upwind scheme, the details of which are available in Roache [22]. Gauss - Seidel iterative procedure is used to solve the resulting algebraic equations. The details of solution procedure are available in Singh and Venkateshan [17]. A 31× 41 cosine function grid in Y-direction and semi-cosine function grids in X-direction for the computational domain is employed. The grid sizes have been fixed based on grid sensitivity test.

## RESULTS AND DISCUSSION

### Code Validation

The computer code, written exclusively for solving the present problem, has been validated, for heat transfer results as given below.

### Justification of velocity boundary conditions used at the opening below the right wall

Three different options are possible for the velocity conditions on the right open boundary, which is a free, inflow or out flow

boundary. A similar study for fixing the velocity boundary condition across the side opening is already done by Singh and Venkateshan [17,18]. First possibility is to assume the vertical velocity (U) is zero, second is to let the cross velocity (V) be zero, and the third is to take the derivatives of U and V in X and Y directions, respectively, to be zero. To see the justification for using the third option of mixed right boundary condition on velocity, the problem has been separately solved with all the three boundary conditions for $q_v = 5\times10^5$ W/ m$^3$, $k_s$ = 0.25 W/ m- K, A = 4, W = 0.5, $N_{rc}$ = $N_{rf}$ = 10.800, ε = 0.85, $\gamma = 1.360$ and $Ra^* = 4.487 \times 10^6$. Here the effects of the three boundary conditions on the flow and temperature fields for the strong radiation case are depicted in Fig 2(a-c).

Figure 2 (a) shows the state of affairs with the boundary condition (I) viz. U = 0 applied across the side opening. The fluid entering through the side opening does not go close to the hot wall. It is diverted away and some of it flows out through the right opening. With the boundary condition (II) applied to the side opening, there is considerable stratification as indicated by Fig. 2(b). Figure 2(c) clearly shows that some of the fluid entering through the side opening travels all the way to the left wall. The isotherm contours for all the three cases are similar near the left and right walls. However, with both boundary condition (I) and (II) the isotherms near the bottom wall show some unusual behavior. The isotherms for the boundary condition (III) indicate a behavior close to that observed by Ramesh et al.[15] in a different geometry. Thus, the boundary condition (III) is the appropriate one along BC.

Table 1 Range of parameters considered in the present study

| Parameters | Range |
|---|---|
| $q_{v,\ W/m^3}$ | $10^5$ - $5\times10^5$ |
| Ra* | $5\times10^4$-$5\times10^6$ |
| $k_{s,\ W/m\text{-}K}$ | 0.25-0.50 |
| γ | 0.6-6 |
| ε | 0.05-0.85 |
| $N_{rc}$, $N_{rf}$ | 8-70 |
| A | 2-4 |
| W | 0.25-0.5 |

**Validation with numerical results Balaji and Venkateshan [11]**

Code validation is possible with the numerical result of Balaji and Venkateshan [11] For comparison, the present geometry is converted to the intermediate fin of a fin array. The side walls are made of a material of finite thermal conductivity and they lose heat from both sides. Local Nusselt number along the extended walls have been compared for the parameters ε = 0, A = 1, Ra = $9.6 \times 10^6$ , $k_s$ = 200 W of a fin array. The side walls are made of a material of finite thermal conductivity and they lose heat from both sides. Local Nusselt number along the extended walls have been compared for the parameters ε = 0, A = 1, Ra = $9.6 \times 10^6$ , $k_s$ = 200 W / m-K, γ = 0.005 with Balaji and Venkateshan [11]. The comparison for these cases termed as good as shown in Fig. 3.

Table 2 Boundary condition justification
$q_v = 5\times 10^5$ W/m$^3$, $Ra^\bullet = 4.487\times 10^6$,
$k_s$ = 0. 25 W/ m K, γ =1.360, $N_{rc}$, $N_{rf}$ = 10.800,
ε = 0.85, A = 4 and W = 0.5.

| Boundary conditions along side opening(BC) | $\theta_{max}$ |
|---|---|
| U = 0 | 0.1668 |
| V =0 | 0.1689 |
| $\frac{\partial U}{\partial X} = \frac{\partial V}{\partial Y} = 0$ | 0.1643 |

**TYPICAL RESULTS FOR SIDE VENTED CAVITIES**

Having validated the present code with previous studies available in the literature, a detailed parametric study has been undertaken. Typical results from this study are presented here for side-vented, open top cavities from highly reflecting to highly emitting walls. The parameter set is taken as shown in Table 1

Figure 4 shows the variation of dimensionless vertical velocity across different sections along the height of the cavity. The velocity profiles show that boundary layers form adjacent to the left and right walls at X = 2 and X = 4. Two peaks are observed, larger one near the heated left wall and a second smaller one close to the right adiabatic wall. Figure clearly shows that the fluid enters across the top opening over more than 50% of the total area.

Figure 5 shows the temperature distributions across different sections of the cavity at X = 0, 2, 4. It is seen that the bottom wall is substantially heated because of radiation whereas the air temperature across a substantial portion of the cavity is at the ambient temperature, except in the boundary layer regions near the left hot wall and the radiantly heated adiabatic right wall.

Figure 6 shows non-dimensional local wall temperature profiles for A = 4, W = 0.5, $q_v = 5\times10^5$ W/m$^3$, $k_s$ = 0.25 W/ m-K and $Ra^* = 4.487\times10^6$ for different surface emissivities. These curves show the effect of surface properties on the wall temperature distribution. It can be seen from Fig. 6 that there is

a monotonic increase in the wall temperature from the cavity bottom to the exit, with the maximum occurring somewhere near the exit of the cavity, in all cases. The sudden small drop in temperature from the maximum in all

cases could probably be due to the abrupt change in the temperature boundary condition to ( $\frac{\partial \theta}{\partial Y} = 0$ ), immediately beyond the exit of the cavity. Figure 6 shows that there is a decrease in wall temperature at any location along the wall with increasing surface emissivity. This is because radiation heat transfer increases with ε for a given set of other parameters and thus brings down the local wall temperature. In the present example, the wall temperature at the cavity exit decreases by 5.7% as emissivity increases from 0.25 to 0.45, and by a further 10.1% with ε increasing to 0.85. Thus, there is substantial decrease in the wall temperature at the cavity exit as one changes the wall surface from a good reflector (like polished aluminium) to a good emitter (like black paint).

Figure 7 shows variation of non-dimensional local wall temperature along the left wall of the cavity with volumetric heat generation and modified Rayleigh number ( Ra*) for A = 4, W = 0.5, $k_s$ = 0.25 W/ m-K and ε = 0.85. These curves show that non-dimensional temperatures decrease with increase in volumetric heat generation and Rayleigh number because $\theta$ is inversely related to $q_v$ as its mathematical form given in nomenclature, but the dimensional wall temperature increases with $q_v$ and Rayleigh number as dimensional wall temperature is directly related to $q_v$.

Figures 8 and 9 show the effects of volumetric heat generation, Rayleigh number and emissivities for the above parameters on maximum non-dimensional and dimensional wall temperatures. As the volumetric heat generation increases, maximum non-dimensional wall temperature decreases but the dimensional wall temperature increases as shown in Figs.8 and 9. The maximum non-dimensional and dimensional wall temperatures always decrease with increase in surface emissivity as explained earlier. The dimensional maximum wall temperature at the exit drops to 12.8% for $q_v = 5\times10^5$ as emissivity increases from 0.05 to 0.85.

The maximum wall temperature decreases with increase in aspect ratio (A) as shown in Fig 10 for the same parameters as above used. Because the right adiabatic wall comes nearer to the left wall as aspect ratio increases and therefore left hot wall
gives more heat to the wall due to surface radiation. So the left wall temperature comes down.

## CORRELATION

Based on a large set of numerical data, a correlation for non dimensional maximum left wall temperature, $\theta_{max}$ is given by

$$\theta_{\max} = 4.850\left(1+Ra^*\right)^{-0.056}\left[\frac{N_{rc}}{1+N_{rc}}\right]^{1.974}\left[\frac{N_{rf}}{1+N_{rf}}\right]^{1.974}$$
$$\left(1+\varepsilon\right)^{-0.528} A^{-1.075}\,\gamma^{0.786}\left(1+W\right)^{0.021} \qquad (12)$$

The exponents of aspect ratio, surface emissivity, conductance parameter and Rayleigh number are negative, which signify that $\theta_{max}$ decreases with increase in all the said parameters. The exponent of (1 + W) is very small and it has a marginal influence on $\theta_{max}$ .

The goodness of fit is indicated by a very high value of correlation coefficient of 0.995 and a standard error of 0.030.

## CONCLUSIONS

The present work is numerically investigated. The local wall temperature at the cavity exit decreases by 5.7% as emissivity increases from 0.25 to 0.45 and by a further 10.1% with emissivity increasing to 0.85. The local maximum wall temperature decreases as aspect ratio increases. The left wall temperature is not significantly affected by change in vent wall. The temperature of the right adiabatic vent wall is always above the ambient temperature causing formation of boundary layer adjacent to the wall.

## REFERENCES


[1]. C. Rodighiero and L. M. de Socio, Some Aspects of Natural Convection in a Corner, *ASME Journal of Heat Transfer*, vol. 105, 1983, pp. 212-214.

[2]. D. Angirisa and R L. Mahajan, Natural Convection from L - Shaped Corners with Adiabatic and Cold Isothermal Walls, *ASME Journal of Heat Transfer*, vol.115,1993, pp.149-157.

[3]. A H. Abib and Y. Jaluria, Numerical Simulation of the Buoyancy –Induced Flow in a Partially Open Enclosure, *Numerical Heat Transfer*, vol.14,1998, pp. 235-254.

[4]. D.M. Kim and R. Viskanta, Effect of Wall Conduction and Radiation on Natural Convection in a Rectangular Cavity, *Numerical Heat Transfer*, 1984, vol. 7, pp. 449-470.

[5]. EI.Hassan Ridouane and H.Mhammed, Effect of Surface Radiation on Multiple Natural Convection Solutions in a Square Cavity Partially Heated from Below, *ASME J. Heat Transfer*, vol. 128, 2006, pp. 1012-1021.

[6]. S.N. Singh, Numerical Study of Laminar Natural Convection in Closed Cavities Heated From Below, accepted for presentation at *International Conference on CAE 07 held at IIT Madras*, 2007,13-15 Dec.

[7]. G. Laurait and G. Desrayaud, Effect of Surface Radiation on Conjugate Natural Convection in Partially Open Enclosures, *International Journal of Thermal Sciences*, vol. 45, 2006, pp. 335-346.

[8]. J.L. Lage, J.S. Lim and A. Bejan, Natural Convection with Radiation in a Cavity with Open Top End, *ASME J. Heat Transfer*, 1992, vol. 114, pp. 479-486.

[9]. C. Balaji and S.P. Venkateshan, Discussion on Natural Convection with Radiation in a Cavity with Open Top end, *ASME Journal of Heat Transfer*, vol. 16(2), 1993, pp. 139-144.

[10]. C. Balaji and S.P. Venkateshan, Interaction of Radiation with Free Convection in an Open Cavity. *International Journal of Heat and Fluid Flow*, vol. 15(4), 1994, pp. 317-324..

[11]. C. Balaji and S.P. Venkateshan, Combined Conduction, Convection and Radiation in a Slot. *International Journal of Heat and Fluid Flow*, vol. 16(2), 1995, pp. 139-144.

[12].A.A. Dehghan and. M.Behnia, Combined Natural Convection, Conduction and Radiation Heat Transfer in a Discretely Heated Open Cavity, *ASME J. Heat Transfer*,.vol.118, 1996, pp.56-64.

[13]. E.Yu and Y.K. Joshi, Heat Transfer in Discretely Heated Side Vented Compact Enclosures by Combined Conduction, Natural Convection and Radiation, *ASME J. Heat Transfer*, vol. 121, 1999, pp. 1002-1010.

[14]. Gururaja Rao, C. Balaji and S.P. Venkateshan, Conjugate Mixed Convection with Surface Radiation from aVertical Plate with a Discrete Heat Source, *ASME J. Heat Transfer*, vol.123, 2001, pp. 698-702.

[15]. N. Ramesh, C. Balaji and S.P. Venkateshan, An Experimental Study of Natural Convection and Surface Radiation in an Open Cavity, *International Journal of Heat and Technology*, vol. 19, 2001, pp. 89-94.

[16]. N. Ramesh. and W. Merzkirch, Combined Convective and Radiative Heat Transfer in Side –Vented Open Cavities, *International Journal of Heat and Fluid Flow*, vol. 22, 2001, pp. 180-187.

[17]. S.N. Singh and S.P. Venkateshan, Numerical Study of Natural Convection with Surface Radiation in Side-Vented Open Cavities, *International Journal of Thermal Sciences*,. vol. 43, 2004, pp.865-876.

[18]. S.N. Singh and S.P. Venkateshan, Natural Convection with Surface Radiation in Partially Open Cavities, *International Journal Heat and Technology*, vol.22 (2), 2004, pp. 57 –64.

[19] C.Gururaja Rao., A. Santosh Kumar., and A.Anand Srinivas.,Effect of Surface Radiation on Conjugate Convection in a Closed and Discretely Heated Rectangular Cavity, *International Journal of Advanced Engineering Technology*, Vol. II, 2011, pp. 172-183.

[20] Samen G. Martyushev., and Mikhail A. Sheremet, Conjugate Natural Convection Combined with Surface Thermal Radiation in an Air Filled Cavity with Internal Heat Source, *International Journal of Thermal Sciences*, Vol. 76,2014, pp.51-67.

[21]. A.D. Gosman, W. M. Pun, A. K. Runchal, D. B. Spalding and M. Wolfshtein, Heat and Mass Transfer in Recirculating Flows, Academic Press, London and New York, 1969.

[22]. P.J. Roache, Computational Fluid Dynamics, Hermosa, *New Mexico*, 1972.

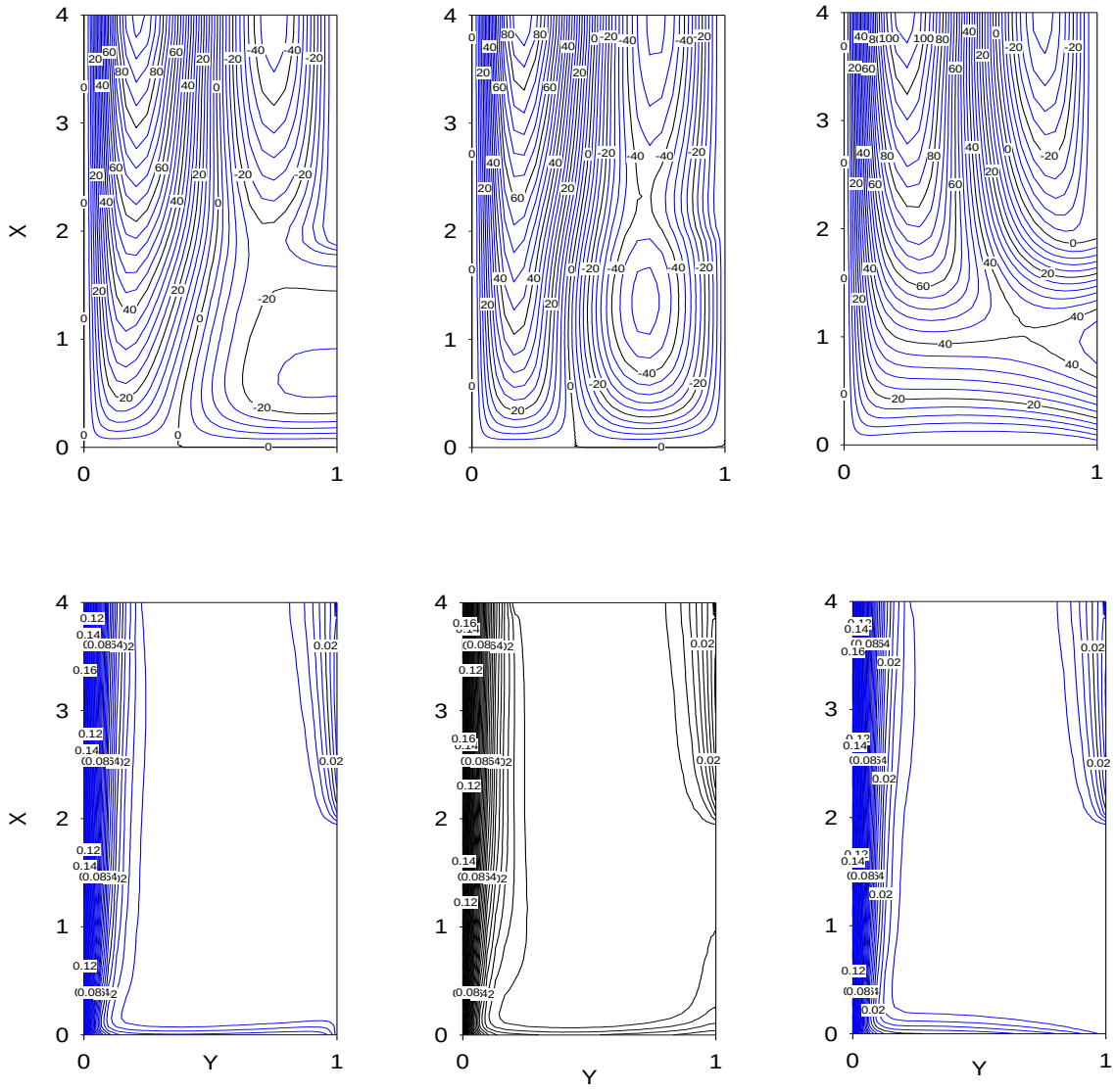


(a) U = 0 (b) V = 0 (c) Mixed velocity b.c

Fig. 2 Streamline and isotherm plots for combined conduction, natural convection and surface radiation with different velocity boundary conditions on the right opening.

[ Top row shows the flow pattern and bottom row gives isotherms]

[$Ra^* = 4.487 \times 10^6$, A = 4, W = 0.5, $\varepsilon = 0.85$, $N_{rc} = N_{rf} = 10.80$ ,

$q_V = 5 \times 10^5$ W/m$^3$, $k_S = 0.25$ W/mK ]

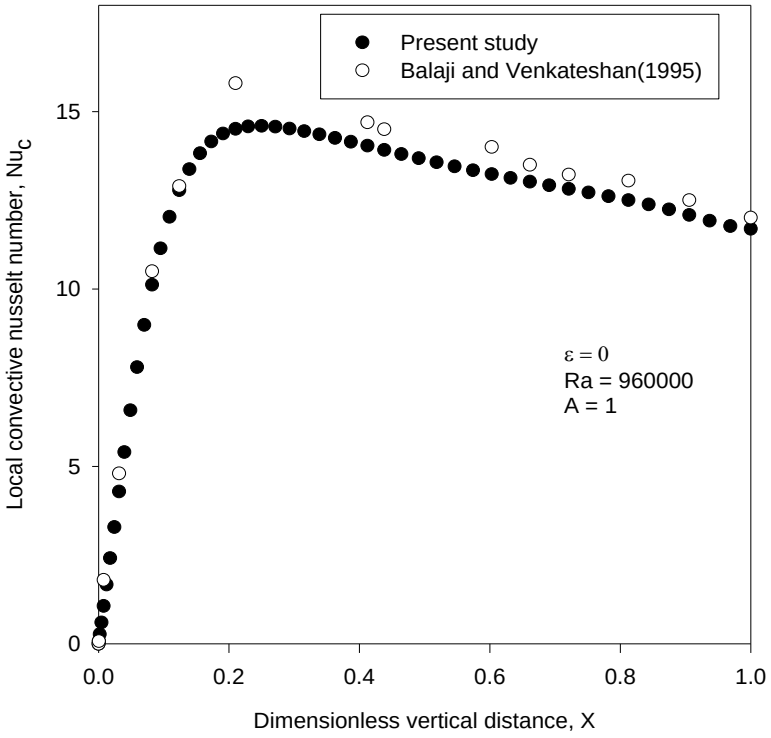


Fig. 3 Convection Nusselt number distribution in the vertical wall of the open cavity for $\varepsilon = 0$

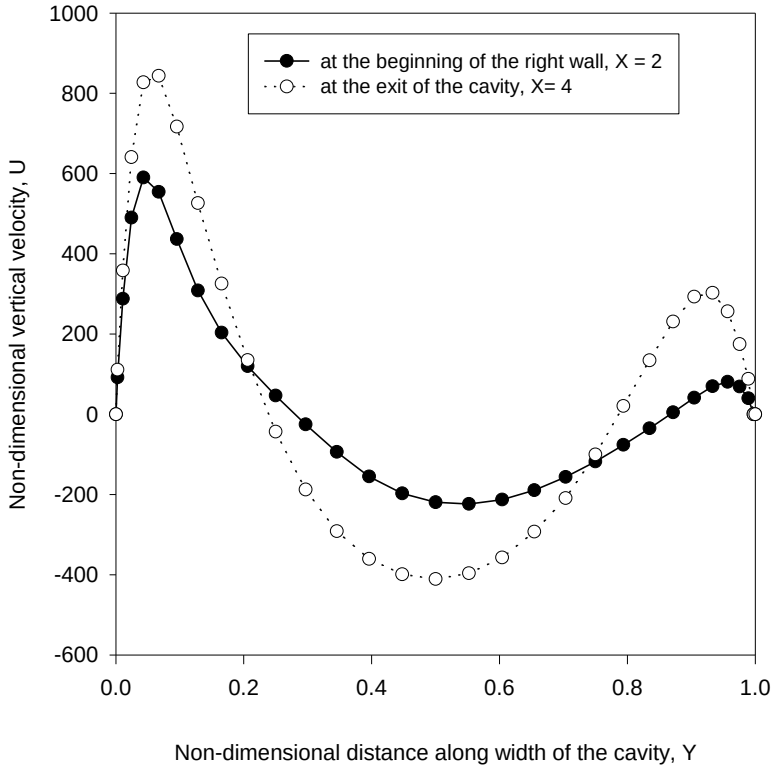


Fig. 4 Non-dimensional vertical velocity distribution at two different sections along the width of the cavity.

[ A = 4, W = 0.5, $q_V$ = 5x10$^5$ W/m$^3$, $k_S$ = 0.25 W/mK, $\varepsilon$ = 0.85 and Ra* = 4.487x10

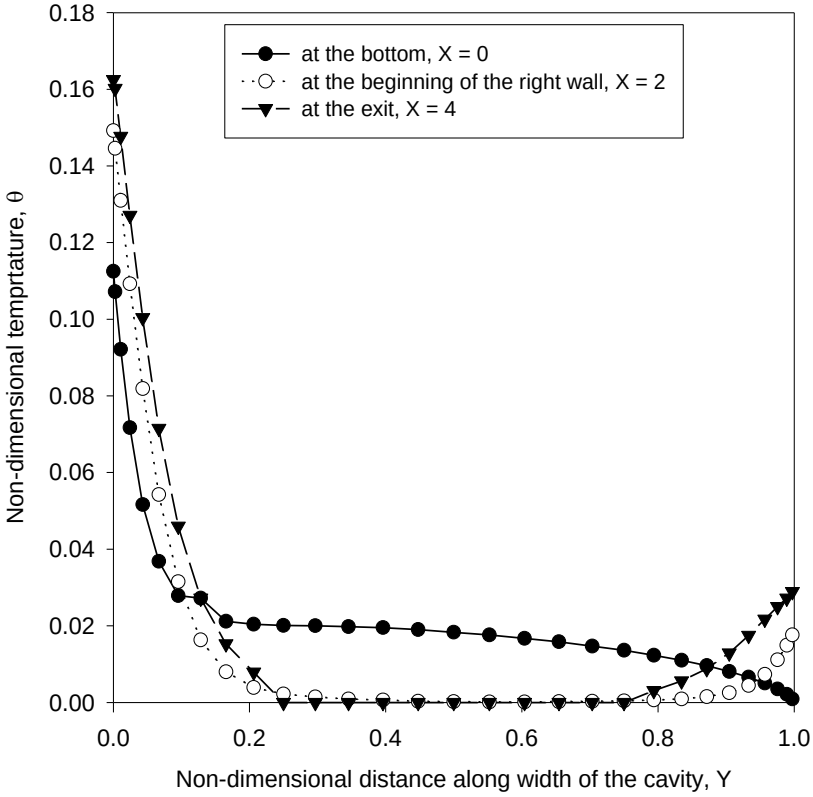


Fig. 5 Non-dimensional temperature distribution at three diffrent sections along the width of the cavity.

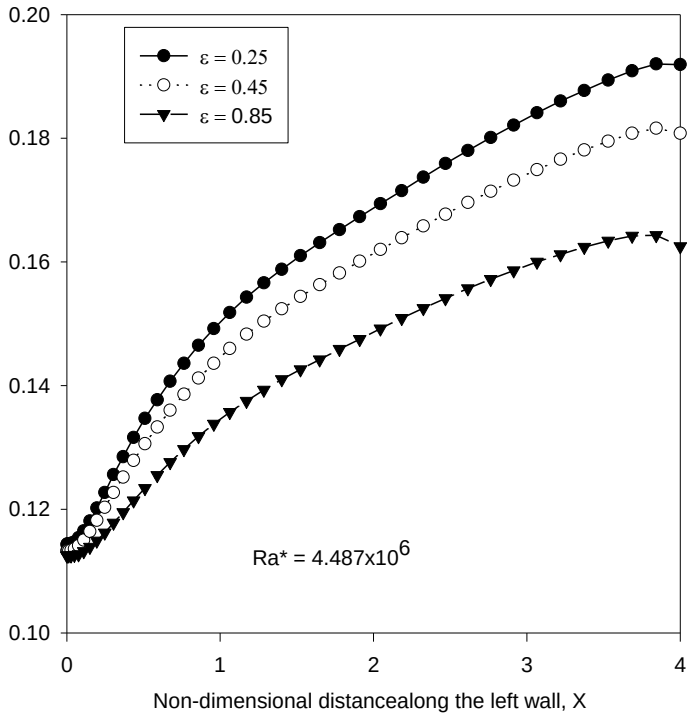


Fig. 6 Non-dimensional local wall temperature profiles for diffrent surface emissivities

[ A = 4, W = 0.5, $q_{v}$ = 5x10$^{5}$ W/m$^{3}$and $k_{s}$ = 0.25 W/mK ]

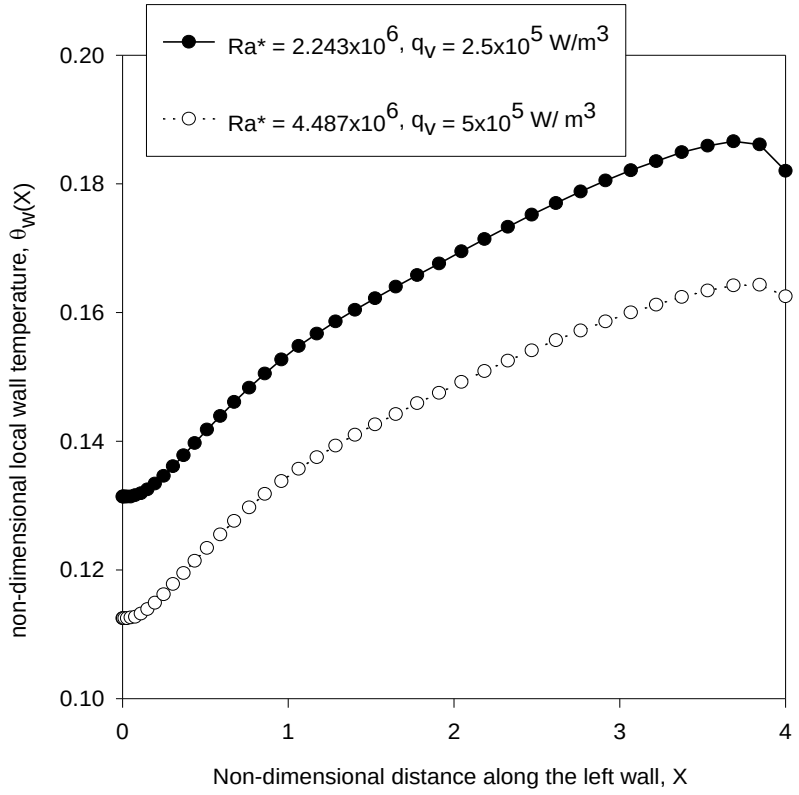


Fig. 7 Non-dimensional local wall temperatureprofiles for two different Rayleigh numbers, (Ra)

[ A = 4, $\varepsilon$ = 0.85, W = 0.5 and $k_S$ = 0.25 W/mK ]

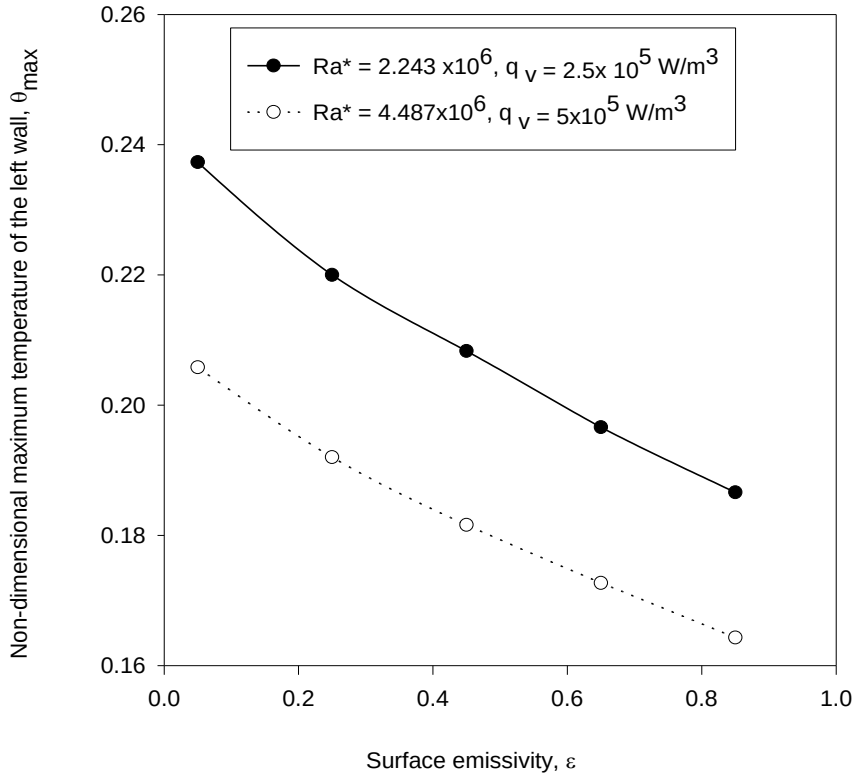


Fig. 8 Non-dimensional maximum wall tempearture at the top of the left wall fordifferent values of Ra*

[ A = 4, W = 0.5 and $K_S$ = 0.25 W /mK ]

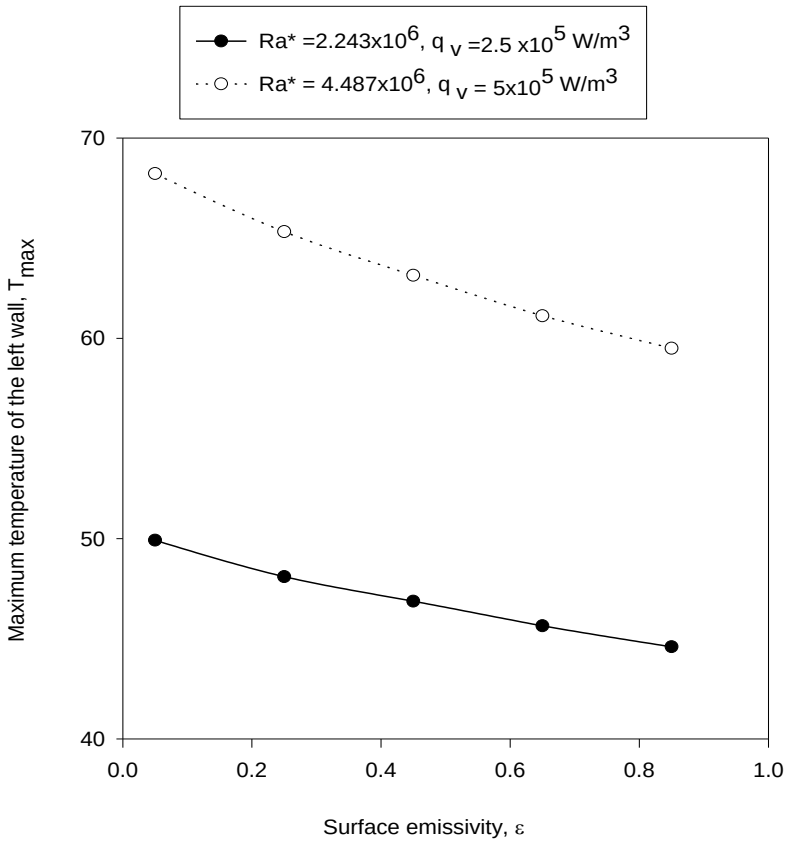


Fig. 9 Dimensional maximum wall temperature at the top of theleft wall for different values of Ra*

[ A = 4, W = 0.5 and $k_S$ = 0.25 W/mk ]

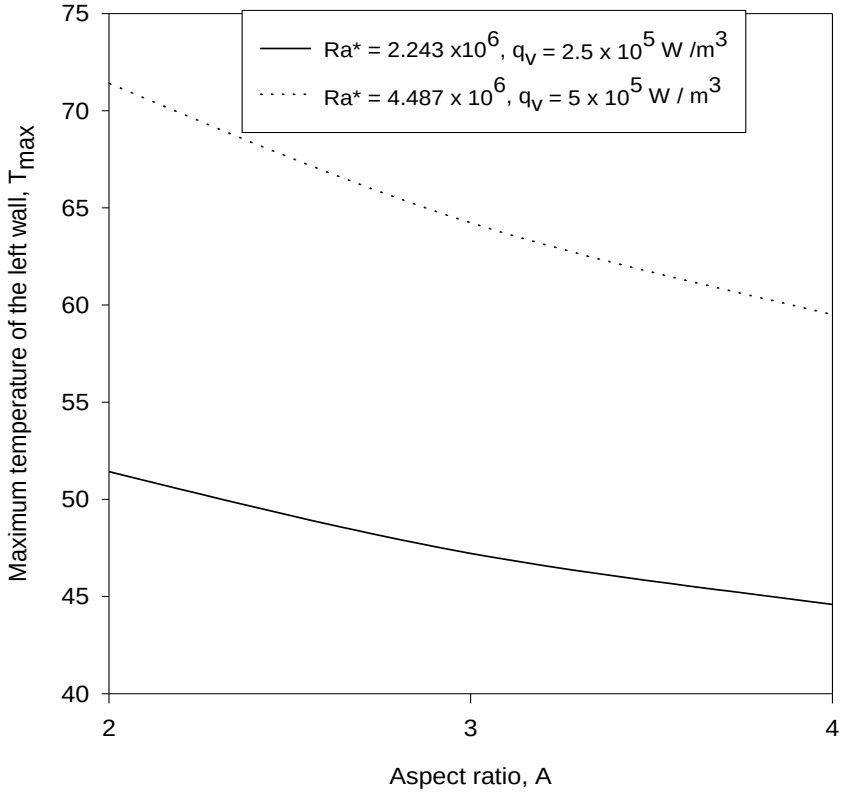


Fig. 10 Dimensional maximum wall temperature at the top of the left wall for the different values of Ra* and $q_V$.

[ ε = 0.85, W = 0.5 and $k_S$ = 0.25 W /mK ]